GSA Data Repository

Tibetan Plateau growth linked to crustal thermal transitions since the Miocene

Xiu-Zheng Zhang[1, 2] Qiang Wang[1, 2*] Derek Wyman [3] Quan Ou[1, 4] Yue Qi[1, 2] Guo-Ning Gou[1] Wei Dan [1, 2] Ya-Nan Yang [1, 2]

[1] *State Key Laboratory of Isotope Geochemistry, Guangzhou Institute of Geochemistry, Chinese Academy of Sciences, Guangzhou, 510640, P. R. China*

[2] *CAS Center for Excellence in Deep Earth Science, Guangzhou, 510640, China*

[3] *School of Geosciences, The University of Sydney, NSW 2006, Australia*

[4] *State Key Laboratory of Oil and Gas Reservoir Geology and Exploitation, Institute of Sedimentary Geology, Chengdu University of Technology, Chengdu 610059, China*

Corresponding Author: * Qiang Wang, E-mail: wqiang@gig.ac.cn

Includes the following Materials

➢ Summary of samples and analysis used in this study

Type	Sample	GPS Position	Host rock	Analysis
Granulite xenoliths	11WL61-7	N: 34°33′21″; E: 90°32′6″	3.8 Ma trachytes	SIMS Zircon U-Pb age SIMS Zircon O isotope Zircon trace elements (ICP-SF-MS) Mineral Chemistry (EPMA) Whole-rock major elements (XRF) Phase Equilibrium
	11WL61-2	N: 34°32′28″; E: 90°32′24″		SIMS Zircon U-Pb age SIMS Zircon O isotope Zircon trace elements (ICP-SF-MS) Mineral Chemistry (EPMA)
Granitic xenolith	11WL61-1-2	N: 34°33′21″; E: 90°32′6″		SIMS Zircon U-Pb age SIMS Zircon O isotope
Amphibolite facies xenoliths	11GM01-20 11GM01-10 11GM01-21	N: 35°01'34" E: 92°40'46"	28 Ma syenites porphyries	Petrography Mineral Chemistry (EPMA) P–T Calculation
Zircon xenocrysts	5123-2	N: 34°25′32″; E: 89°7′39″	2.3Ma dacite	SIMS Zircon U-Pb age SIMS Zircon O isotope
Zircon xenocrysts	13SW16-1	N: 33°46'15" E: 90°15'14"	~6 Ma trachydacites	LA-ICP-MS Zircon U-Pb age SIMS Zircon O isotope
	13SW20-1	N: 33°45'22" E: 90°20'16"		
	13SW02-1	N: 33°51'32" E: 90°21'59"		
	13SW47-1	N: 33°46'06" E: 90°15'13"		
	13SW49-1	N: 33°39'33" E: 90°18'32"		
	14QW326-2	N: 33°49'32.5" E: 90°39'07.5"		
	14QW328-3	N: 33°48'43.8" E: 90°33'55.1"		

Text S1. Analytical methods

1. Phase Equilibrium

P–T pseudosection has been calculated for the granulite sample 11WL61-7 in the NCKFMASHTO (Na_2O–CaO–K_2O–FeO–MgO–Al_2O_3–SiO_2–H_2O–TiO_2–Fe_2O_3) system using the software THERMOCALC, version 3.40i (Powell and Holland, 1988) (updated February, 2012). The whole-rock composition of 11WL61-7 was analyzed on fused glass beads using a Rigaku RIX 2000 X-ray fluorescence (XRF) spectrometer at the State Key Laboratory of Isotope Geochemistry, Guangzhou Institute of Geochemistry, Chinese Academy of Sciences. Analytical uncertainties are between 1% and 5%. The input bulk composition is: SiO_2 = 52.23 (wt.%), Al_2O_3 = 15.93 (wt.%), TiO_2 = 0.83 (wt.%), Fe_2O_3 = 8.48 (wt.%), MnO = 0.08 (wt.%), MgO = 6.33 (wt.%), CaO = 8.15(wt.%), Na_2O = 2.49 (wt.%), K_2O = 2.05 (wt.%) and P_2O_5 = 0.20 (wt.%). These oxides were normalized in the NCKFMASHTO system by assuming that P_2O_5 is present in apatite and the O (Fe_2O_3) value equals to the summation of the Fe^{3+} content in each constituent mineral calculated by charge balance constraints (Fe^{3+}/ (Fe^{2+}+ Fe^{3+}) ≈ 0.1). Except where H_2O is considered as a compositional variable, the modelled bulk-rock water contents were adjusted according to Palin et al. (2016): minimal free fluid (~1 mol.%) was present at the 8-kbar solidus to ensure that the solidus remained fluid-saturated over the entire P-T range of interest. The mineral activity–composition relationships are as follows: metabasite melt, clinopyroxene and amphibole (Green et al., 2016); garnet, orthopyroxene, biotite and chlorite (White et al., 2014); olivine and epidote (Holland and Powell, 2011); magnetite–spinel (White et al., 2002); ilmenite–hematite (White et al., 2000); plagioclase and K-feldspar (Holland and Powell, 2003); and muscovite–paragonite (White et al., 2014). Pure phases included quartz, rutile, titanite and aqueous fluid (H_2O).

2. Zircon U-Pb age analysis

Zircon grains were separated from fresh samples using conventional heavy liquid and magnetic techniques and then hand-picked under a binocular microscope. They were casted in the epoxy mount and polished to about half their thickness for analysis. Cathodoluminescence (CL) images of zircons were conducted at State Key Laboratory of Isotope Geochemistry, Guangzhou Institute of Geochemistry, Chinese Academy of Sciences (SKLaBIG GIGCAS).

2.1 SIMS

Zircon U-Pb analyses were conducted using the Cameca IMS 1280HR secondary ion mass spectrometry (SIMS) with a spot size of 20×30 μm at the SKLaBIG GIGCAS. Analytical procedures are similar to those described by Li et al. (2009). An O_2^- primary ion beam with an intensity of ~10 nA was accelerated at -13kV. The aperture illumination mode was used with a 200 μm primary beam mass filter aperture to produce even sputtering over the entire analyzed area. The secondary ion beam optics was optimized to achieve a mass resolution of about 5400 to separate Pb^+ peaks from isobaric interferences. Rectangular lenses were activated to increase the transmission at high mass resolution. A single electron multiplier was used in ion-counting mode to collect secondary ions by switching the magnetic field following the peak jumping sequence: 196 ($^{90}Zr_2{}^{16}O$, matrix reference), 200 ($^{92}Zr_2{}^{16}O$), 200.5 (background), 203.81 ($^{94}Zr_2{}^{16}O$, for mass calibration), 203.97 (^{204}Pb), 206 (^{206}Pb), 207 (^{207}Pb), 208 (^{208}Pb), 209 ($^{177}Hf^{16}O_2$), 238 (^{238}U), 248 ($^{232}Th^{16}O$), 270 ($^{238}U^{16}O_2$), and 270.1 (reference mass). The integration time for these mass are1.04, 0.56, 4.16, 0.56, 6.24, 4.16, 6.24, 2.08, 1.04, 2.08, 2.08, 2.08, and 0.24 s, respectively. Each measurement consisted of seven cycles, and the total analytical time per measurement was ~12 minutes.

Zircon U–Th–Pb isotopic ratios were corrected using the standard zircon Plešovice (Sláma et al., 2008) based on a power low relationship between measured $^{206}Pb^+/^{238}U^+$ and $^{238}U^{16}O_2^+/^{238}U^+$. The ^{207}Pb-based common lead correction was used to derive the U-Pb ages (Age^{207c} in Table S1) with a present-day crustal composition of $^{207}Pb/^{206}Pb_{common}$ = 0.84 for the common Pb. A long-term uncertainty of 1.5% (1 RSD) for $^{206}Pb/^{238}U$ measurements of the standard zircons was propagated to the unknowns (Li et al., 2010), despite that the measured $^{206}Pb/^{238}U$ error in a specific session is generally around 1% (1 RSD) or less. Data reduction was carried out using the Isoplot/Ex v. 3.0 program (Ludwig, 2003). Uncertainties on individual analyses in the data tables are reported at a 1σ level. Mean ages for pooled U/Pb and Pb/Pb analyses are quoted with 2σ and/or 95% confidence intervals. In this study, we analyzed six Qinghu grains yielding a concordia age of 160.1 ± 2.0 Ma, which is identical to the recommended value of 159.5 ± 0.2 Ma (Li et al., 2013) within analytical uncertainties.

2.1 LA-ICP-MS

Zircon U-Pb dating was performed using LA-ICP-MS for zircon xenocrysts contained in ~6 Ma trachydacites at the Institute of Geology and Geophysics, Chinese Academy of Sciences (Table S2). An Agilent 7500a quadruple (Q)–ICPMS and a Neptune multi-collector (MC)–ICPMS with a 193 nm excimer ArF laser-ablation system (GeoLas Plus) were used for determination of zircon U–Pb ages. The analyses were conducted with a spot diameter of 40 μm with a typical ablation time of approximately 30 s for 200 cycles of each measurement, an 8 Hz repetition rate, and a laser power of 100mJ/pulse. Zircon 91500 was used as the standard (Wiedenbeck et al., 1995) and the standard silicate glass NIST 610 was used to optimize the machine. $^{207}Pb/^{206}Pb$ and $^{206}Pb/^{238}U$ ratios were calculated using the GLITTER program (Jackson et al., 2004). Common Pb was corrected by ComPbCorr#3 151 (Andersen, 2002) for those with common^{206}Pb > 1%. The weighted mean ages are quoted at the 95% confidence level. The age calculations and concordia plots were made using Isoplot (ver 3.0) (Ludwig, 2003).

3. Zircon O isotope compositions

Zircon oxygen isotopes were measured using Cameca IMS 1280HR SIMS at SKLaBIG GIGCAS. The detailed analytical procedures were similar to those described by Li et al. (2009). The measured oxygen isotopic data were corrected for instrumental mass fractionation (IMF) using the Penglai zircon standard ($\delta^{18}O_{VSMOW}$ = 5.3 ‰) (Li et al., 2009). The internal precision of a single analysis generally was better than 0.2 ‰ (1σ) for the $^{18}O/^{16}O$ ratio. The external precision, measured by the reproducibility of repeated analyses of the Penglai standard, is 0.10 ‰ (2σ, n = 24). Eight measurements of the Qinghu zircon standard during the course of this study yielded a mean of $\delta^{18}O$ = 5.51 ± 0.20 ‰ (2σ), which is consistent within analytical errors with the reported value of 5.4 ± 0.2 ‰ (Li et al., 2013)(Tables S1, S2).

4. Zircon Trace Element

In situ trace element for the zircon of granulite xenoliths were measured with an ELEMENT XR (Thermo Fisher Scientific) ICP-SF-MS coupled with a 193-nm (ArF) Resonetics RESOlution M-50 laser ablation system in the SKLaBIG GIG CAS. Laser condition was set as following: beam size, 33μm; repetition rate, 6Hz; energy density, ~4 J cm^{-2}. A smoothing device (The Squid, Laurin Technic) was used to smooth the sample signal. Each spot analysis consisted of 20 s gas blank collection with the laser off, and 30 s sample signal detection with the laser on. Si was selected as the internal standard element. NIST610 was selected as the calibration standard. The oxide molecular yield, indicated by the $^{232}Th^{16}O/^{232}Th$ ratio, was less than 0.3%. The detailed experiment procedure and data reduction strategy are described in Zhang et al. (2019). NIST612 was measured as unknown samples. 30 analyses of NIST612 indicate most elements are within 8% of the reference values and the analytical precision (2RSD) was better than 10% for most elements (Table S3).

5. Mineral Chemistry

Representative minerals in the crustal xenoliths were selected for chemical analysis by electron probe micro-analyzer (EPMA) JEOL JXA-8800 at the SKLaBIG GIG CAS. The operating conditions were 20 kV, 20 nA beam current, and 5 μm probe diameter. Representative mineral analyses are listed in Tables S4 and S5. The structural formulae have been given for fixed oxygen values and with Fe^{3+} calculated by stoichiometric charge balance.

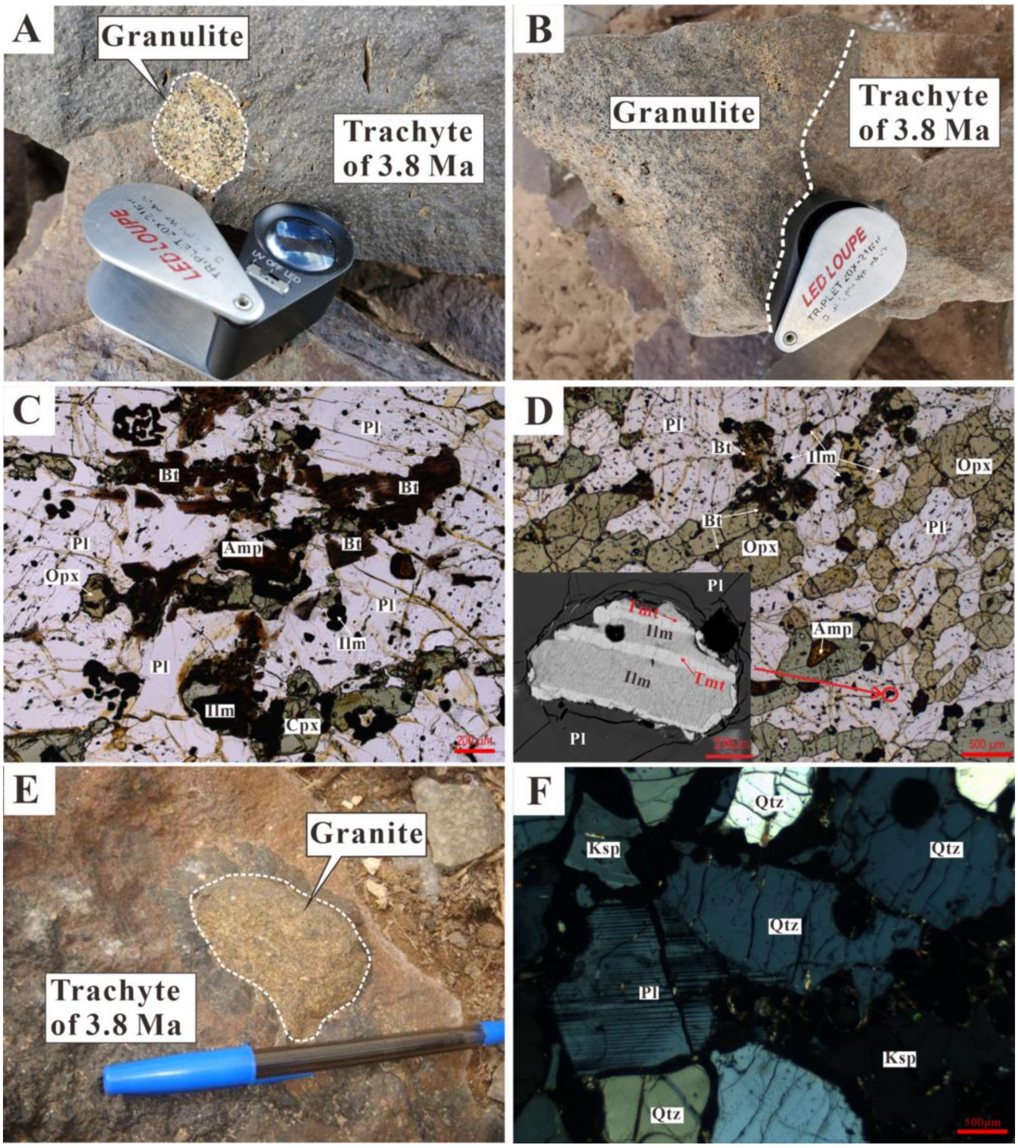

Figure S1 Field photographs and photomicrographs of the crustal xenoliths contained in 3.8 Ma trachyte, from Wulanwulahu area, central Tibet. (A-B) Field photographs showing the occurrences of the granulite xenoliths. (C) Photomicrographs of mafic granulite xenoliths 11WL61-2 (plane polarized light photomicrograph). (D) Granulite samples 11WL61-7 exhibit foliation defined by the preferred orientation of mineral grains. Minor titanomagnetite was observed to occurred as parallel lamellae within ilmenite. (E-F) Field photographs and photomicrographs of the granitic xenoliths. Amp = amphibole, Pl = plagioclase, Bt = biotite, Opx = orthopyroxene, Cpx = clinopyroxene, Ksp = K-feldspar, Qtz = quartz, Ilm = ilmenite, Tmt = titanomagnetite

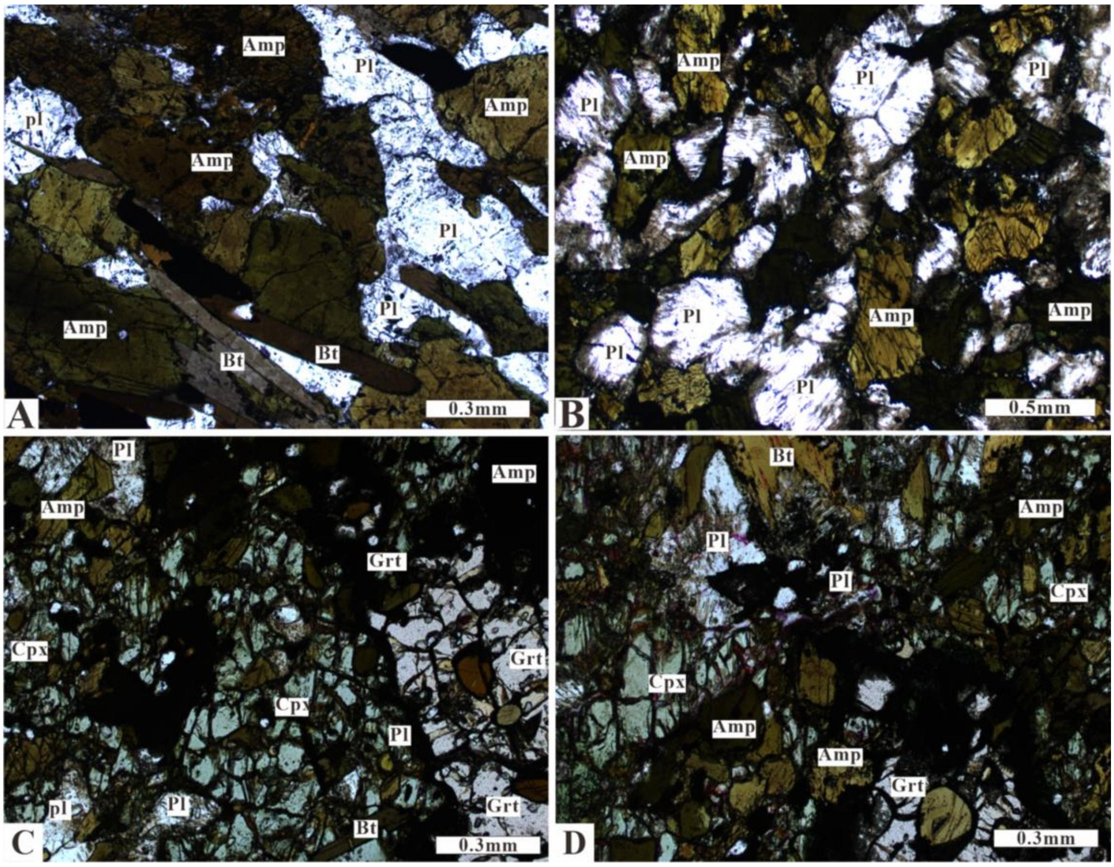

Figure S2 Photomicrograph (plane polarized light) showing the mineral textures and mineral assemblage of crustal xenoliths contained in 28 Ma syenites porphyries. (A-B) amphibolite (C-D) garnet amphibolite. These xenoliths have medium-grained polygonal granoblastic texture with the assemblages of amphibole (35–50 vol. %) + plagioclase (35–40 vol. %) + biotite (5–10 vol. %) + quartz (5–7 vol. %) + ilmenite (0–5 vol. %) + garnet (0–8 vol. %) + clinopyroxene (0–7 vol. %). Compared with the water-poor granulite xenoliths, these amphibolite facies crustal xenoliths are rich in hydrous minerals (e.g., biotite and amphibole), up to 40–60 vol. %. Amp = amphibole, Pl = plagioclase, Bt = biotite, Grt = garnet, Cpx = clinopyroxene.

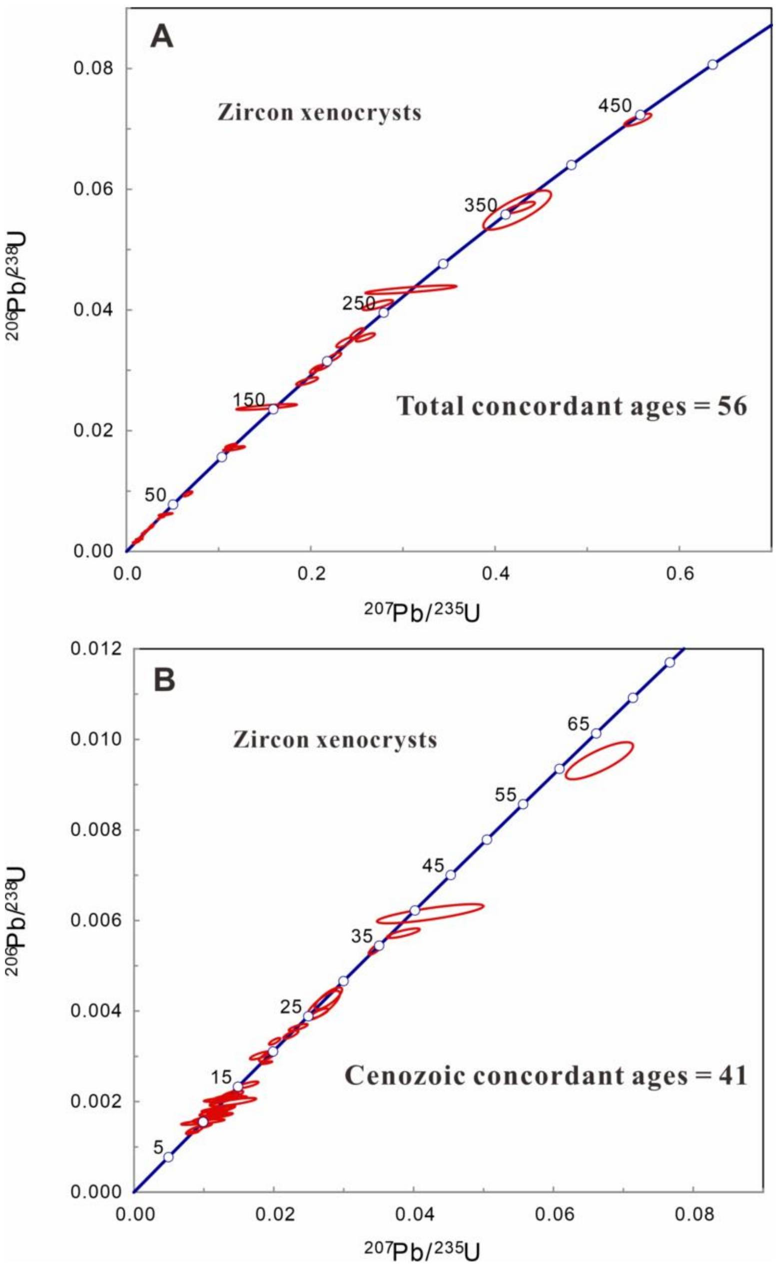

Figure S3 U–Pb concordia diagrams for the zircon xenocrysts from 6–2.3 Ma lavas. Eight samples displayed clear oscillatory zoning of magmatic origin and yielded 56 concordant U–Pb ages (from 81 analyses) of 445–8.5 Ma (Tables S2), with most (41 analyses, 73%) being of Cenozoic age.

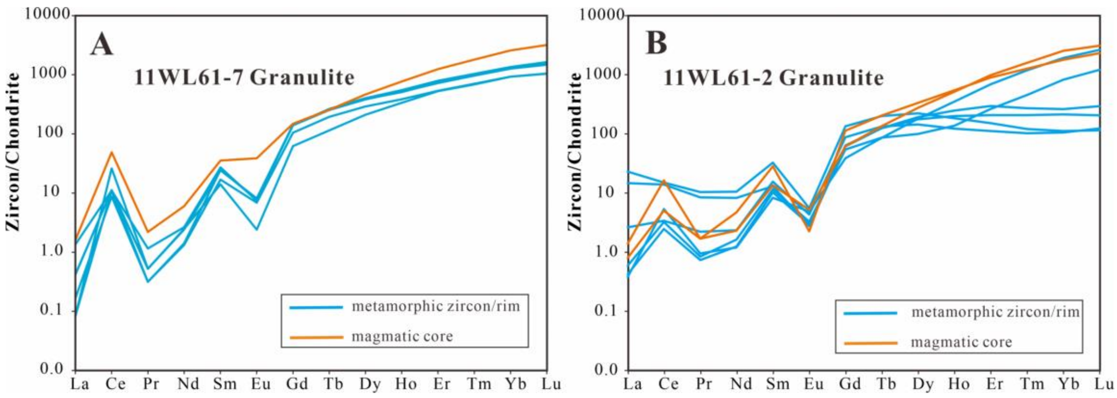

Figure S4 Chondrite normalised REE patterns of zircon cores and metamorphic overgrowths from granulite xenoliths contained in 3.8 Ma trachyte. Chondrite values are from Sun and McDonough (1989).

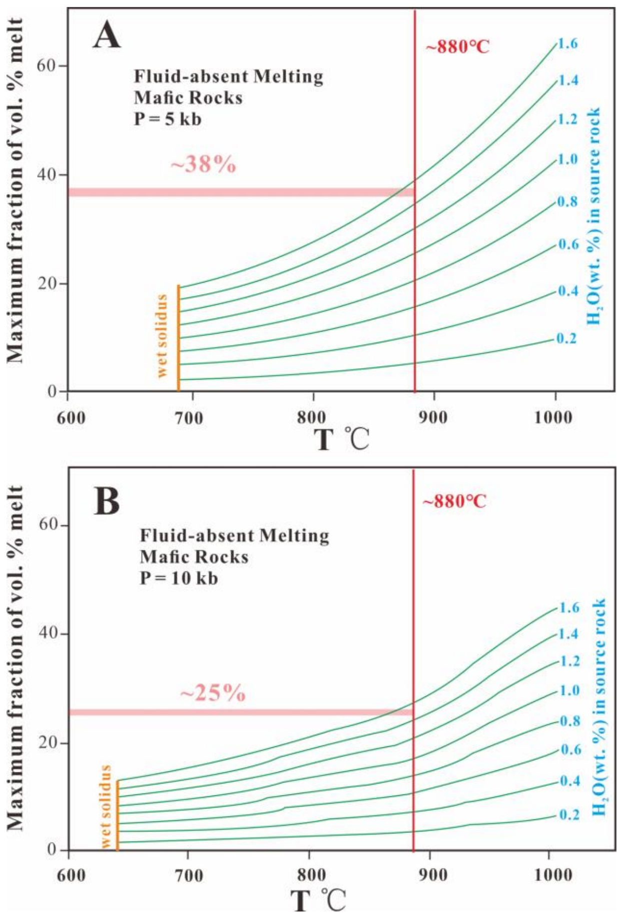

Figure S5 Diagram showing the amounts of melt formed from fluid-absent reactions in mafic rocks at (A) 5 kbar and (B) 10 kbar as a function of temperature and water content of the source rock (Clemens et al., 1987). These diagrams can be used to estimate roughly the amount of melt produced during the thermal transition from the amphibolite-facies crust of 28 Ma to the granulite-facies crust of 22.6–12.9 Ma. The original H_2O-rich middle crust (~1.5 wt.% H_2O) at 28 Ma could produce as much as 25–38 vol. % melts during 22.6–12.9 Ma when the temperature rose to 880℃, which is consistent with the results of phase equilibrium (Figs. 2D). The H_2O contents (~1.5 wt.%) are calculated based the mineral assemblages (vol. %, $Amp_{40}Pl_{35}Bt_{10}Cpx_{8}Grt_{7}$) and mineral properties (see blow, Hacker et al. 2004).

	Pl	**Grt**	**Cpx**	**Amp**	**Bt**
Density (g/cm^3)	2.7	4.31	3.26	3.24	2.79
H_2O (wt.%)	0	0	0	2.5	4.5

Table S1 SIMS zircon U-Pb and O isotopic results of crustal xenoliths entrained in 3.8 Ma trachytes.

Spot #	Properties	U (ppm)	Th (ppm)	Pb (ppm)	Th/U	$^{238}U/^{206}Pb$	±1σ (%)	$^{207}Pb/^{206}Pb$	±1σ (%)	Age^{207c} (Ma)	±1σ	$\delta^{18}O$	1σ
11WL61-7: granulite xenolith													
1	metamorphic	698	90.6	2.39	0.13	320.88	1.64	0.04832	2.83	20.0	0.3	12.16	0.09
2	metamorphic	494	52.6	1.89	0.11	280.47	2.13	0.04959	2.28	22.9	0.5	12.52	0.12
3	metamorphic	793	129	2.93	0.16	283.11	2.44	0.06150	2.13	22.3	0.5	12.18	0.11
4	metamorphic	2039	107	7.69	0.05	280.43	1.99	0.04629	1.30	23.0	0.5	12.64	0.13
5	metamorphic	723	101	2.64	0.14	300.94	2.54	0.04884	2.51	21.3	0.5	12.25	0.14
6	metamorphic	704	72.2	2.36	0.10	319.88	1.92	0.05082	3.82	20.0	0.4	11.84	0.09
7	core	938	1058	52.5	1.13	25.30	1.53	0.05317	0.60	249.2	3.8	5.94	0.12
8	rim	814	129	2.0	0.16	267.24	2.71	0.16676	5.05	20.4	0.6	12.26	0.11
11WL61-2: granulite xenolith													
1	rim	2420	45.8	6.57	0.02	380.46	1.53	0.05253	1.63	16.8	0.3	9.88	0.11
2	rim	2749	47.0	5.0	0.02	490.62	1.68	0.05141	1.75	13.0	0.2	10.15	0.11
3	rim	2906	61.6	7.0	0.02	401.68	1.62	0.04950	2.33	16.0	0.3	10.15	0.12
4	rim	3057	67.3	8.07	0.02	394.58	1.61	0.04996	2.37	16.2	0.3	10.06	0.11
5	core	403	315	15.3	0.78	32.98	1.63	0.05182	1.39	192.1	3.1	6.07	0.15
6	core	415	76.8	54.0	0.18	8.66	1.52	0.06531	0.50	702.6	10.4	5.23	0.12
7	rim	1455	60.6	4.30	0.04	368.28	1.73	0.05285	1.48	17.3	0.3	10.53	0.13
8	metamorphic	2264	37.7	4.79	0.02	494.79	1.57	0.04814	1.67	13.0	0.2	9.69	0.08
9	metamorphic	1916	21.0	3.98	0.01	502.51	1.62	0.05199	1.51	12.7	0.2	10.36	0.15
11WL61-1-2: granitic xenolith													
1	magmatic	22930	1501	37	0.07	666.17	2.97	0.04748	0.46	9.65	0.29	9.16	0.15
2	magmatic	5284	383	8	0.07	684.71	2.45	0.04935	1.06	9.37	0.23	9.39	0.23
3	magmatic	2906	111	4	0.04	693.70	1.51	0.04698	2.24	9.28	0.14	9.23	0.23
4	magmatic	7364	375	11	0.05	718.34	2.39	0.04790	1.10	8.95	0.21	9.23	0.19
5	magmatic	6439	403	10	0.06	683.77	1.50	0.04807	1.37	9.40	0.14	9.23	0.11
6	magmatic	5535	175	9	0.03	671.01	2.35	0.05010	1.03	9.55	0.22	9.29	0.12
7	magmatic	10670	966	16	0.09	712.34	1.59	0.04900	0.74	9.01	0.14	9.62	0.14
8	magmatic	4661	129	6	0.03	783.48	1.50	0.04765	1.18	8.21	0.12	9.23	0.16
9	magmatic	5517	158	8	0.03	754.99	1.66	0.04742	1.27	8.52	0.14	9.46	0.24

10	magmatic	3586	93	5	0.03	748.21	1.54	0.04736	1.44	8.60	0.13	9.77	0.15
11	magmatic	6303	476	9	0.08	724.86	1.57	0.04740	0.99	8.87	0.14	9.03	0.16

Zircon U-Pb： Qinghu zircon standard, Concordia age = 160.1 ± 2.0 Ma

Sample/ spot #	[U] ppm	[Th] ppm	Th/U meas	$^{207}Pb/^{235}U$	±σ %	$^{206}Pb/^{238}U$	±σ %	ρ	$^{207}Pb/^{235}U$	±σ	$^{206}Pb/^{238}U$	±σ
QH@01	1152	448	0.388	0.17079	1.59	0.0251	1.50	0.94850	160.1	2.4	159.6	2.4
QH@02	1620	741	0.457	0.17128	1.57	0.0251	1.50	0.95548	160.5	2.3	160.0	2.4
QH@03	1369	729	0.532	0.16990	1.59	0.0248	1.51	0.94717	159.3	2.3	158.0	2.4
QH@04	1229	504	0.410	0.17179	1.86	0.0252	1.54	0.82890	161.0	2.8	160.2	2.4
QH@05	966	506	0.524	0.16886	1.70	0.0245	1.56	0.91276	158.4	2.5	156.3	2.4
QH@06	1306	613	0.469	0.17662	1.70	0.0260	1.58	0.92768	165.1	2.6	165.2	2.6

Zircon oxygen isotopes： Qinghu zircon standard, mean of $\delta^{18}O$ = 5.51 ± 0.20 ‰ (2σ)

	QH@01	QH@02	QH@03	QH@04	QH@05	QH@06	QH@07	QH@08
$\delta^{18}O$	5.47	5.47	5.71	5.39	5.56	5.46	5.57	5.47
1σ	0.14	0.11	0.16	0.17	0.10	0.07	0.13	0.14

Note: Age^{207c} is $^{206}Pb/^{238}U$ age which common Pb was corrected by ^{207}Pb-correction method.

Table S2 LA-ICP-MS U-Pb isotopic and SIMS O isotopic data of zircon xenocrysts in 6.0–2.3 Ma lavas.

Spot	Th (ppm)	U (ppm)	Th/U	$^{207}Pb/^{206}Pb$		$^{207}Pb/^{235}U$		$^{206}Pb/^{238}U$		$^{207}Pb/^{206}Pb$ (Ma)		$^{207}Pb/^{235}U$ (Ma)		$^{206}Pb/^{238}U$ (Ma)		δ18O	1σ	Disc
				$^{207}Pb/^{206}Pb$	1σ	$^{207}Pb/^{235}U$	1σ	$^{206}Pb/^{238}U$	1σ	Age	1σ	Age	1σ	Age	1σ			
SIMS U-Pb isotopic data of zircon xenocrysts from 2.3 Ma dacite																		
5123-2@01	3512	87	0.01	0.04719	0.00129	0.02783	0.00129	0.00428	0.00016	59.0	63.9	27.9	1.3	27.5	1.0	9.81	0.09	1%
5123-2@02	4185	86	0.00	0.04761	0.00145	0.02709	0.00158	0.00413	0.00021	79.8	70.9	27.1	1.6	26.5	1.3	9.42	0.10	2%
5123-2@03	9541	225	0.03	0.04662	0.00046	0.03453	0.00063	0.00537	0.00008	29.8	23.7	34.5	0.6	34.5	0.5	8.75	0.17	0%
5123-2@05	331	199	0.52	0.05041	0.00187	0.19601	0.00785	0.02820	0.00043	214.1	83.7	181.7	6.7	179.3	2.7	6.15	0.18	1%
5123-2@07	856	754	0.82	0.05069	0.00093	0.22492	0.00534	0.03218	0.00049	226.8	41.8	206.0	4.4	204.2	3.0	6.74	0.13	1%
5123-2@08	240	223	0.01	0.06488	0.00669	0.01255	0.00136	0.00140	0.00005	770.6	203.1	12.7	1.4	9.0	0.3	8.96	0.12	40%
5123-2@10	358	174	0.58	0.04966	0.00102	0.23706	0.00614	0.03463	0.00055	178.9	47.0	216.0	5.0	219.4	3.4	7.59	0.18	-2%
5123-2@11	208	171	0.01	0.06797	0.00872	0.00899	0.00120	0.00096	0.00003	867.7	245.4	9.1	1.2	6.2	0.2	8.32	0.14	47%
5123-2@12	3806	344	0.05	0.04680	0.00125	0.02245	0.00071	0.00348	0.00006	39.3	62.8	22.5	0.7	22.4	0.4	7.09	0.15	1%
5123-2@13	2868	480	(0.03)	0.04384	0.00094	0.02012	0.00053	0.00333	0.00005	-119.7	52.2	20.2	0.5	21.4	0.3	6.58	0.18	-6%
5123-2@14	590	20	0.00	0.05505	0.00445	0.01081	0.00091	0.00142	0.00003	414.2	171.3	10.9	0.9	9.2	0.2	11.66	0.20	19%
5123-2@15	603	557	0.81	0.15816	0.00076	8.30794	0.15137	0.38099	0.00670	2436.0	8.1	2265.2	16.6	2080.9	31.3	10.87	0.18	17%
5123-2@16	855	383	0.49	0.05018	0.00063	0.25010	0.00492	0.03615	0.00055	203.5	29.1	226.7	4.0	228.9	3.4	8.07	0.20	-1%
5123-2@17	886	110	0.01	0.05171	0.00227	0.01712	0.00081	0.00240	0.00004	272.5	97.6	17.2	0.8	15.5	0.3	6.53	0.14	11%
5123-2@18	2622	106	0.00	0.04956	0.00159	0.01466	0.00063	0.00215	0.00006	174.5	73.0	14.8	0.6	13.8	0.4	8.42	0.20	7%
5123-2@19	2406	153	0.06	0.04607	0.00156	0.01912	0.00081	0.00301	0.00008	0.0	81.2	19.2	0.8	19.4	0.5	8.16	0.12	-1%
5123-2@20	1616	272	0.03	0.04861	0.00129	0.02651	0.00086	0.00395	0.00007	129.1	61.4	26.6	0.9	25.4	0.5	6.91	0.13	4%
5123-2@21	350	143	0.02	0.05209	0.00628	0.01295	0.00162	0.00180	0.00006	289.5	254.4	13.1	1.6	11.6	0.4	6.45	0.21	13%
LA-ICP-MS U-Pb isotopic data of zircon xenocrysts from ~6 Ma trachyte																		
13SW16-1 02	948	1490	0.64	0.06166	0.00638	0.01471	0.00130	0.00184	0.00005	662	142	15	1	11.8	0.3	7.52	0.1	27%
13SW16-1 06	493	1608	0.31	0.05901	0.00370	0.02132	0.00127	0.00271	0.00006	567	92	21	1	17.4	0.4	9.55	0.1	21%
13SW16-1 08	1718	2884	0.60	0.04606	0.00721	0.01308	0.00203	0.00206	0.00004	1	281	13	2	13.3	0.2	9.87	0.1	-2%
13SW16-1 09	2231	1493	1.49	0.04736	0.00456	0.01068	0.00087	0.00175	0.00004	67	133	10.8	0.9	11.3	0.3	8.97	0.13	-4%
13SW16-1 13	2216	2244	0.99	0.04733	0.00608	0.01196	0.00151	0.00183	0.00004	66	256	12	2	11.8	0.3	8.84	0.1	2%
13SW16-1 14	504	4683	0.11	0.04682	0.00182	0.02349	0.00089	0.00364	0.00005	40	57	23.6	0.9	23.4	0.3	8.78	0.09	1%

13SW16-1 20	330	1275	0.26	0.05550	0.00482	0.01195	0.00086	0.00172	0.00004	433	115	12.1	0.9	11.1	0.3	7.92	0.09	9%
13SW20-1 03	724	1105	0.66	0.04605	0.00250	0.01074	0.00053	0.00169	0.00004		118	10.8	0.5	10.9	0.2			-1%
13SW20-1 04	718	7500	0.10	0.05286	0.00252	0.01023	0.00046	0.00140	0.00002	323	111	10.3	0.5	9	0.1			14%
13SW20-1 07	2069	3079	0.67	0.04361	0.00231	0.01807	0.00098	0.00302	0.00006	-91	81	18.2	1	19.5	0.4			-7%
13SW20-1 09	504	661	0.76	0.05522	0.01238	0.01386	0.00305	0.00182	0.00008	421	436	14	3	11.7	0.5			20%
13SW20-1 11	728	4677	0.16	0.05296	0.00511	0.00822	0.00076	0.00113	0.00003	327	221	8.3	0.8	7.3	0.2			14%
13SW20-1 14	1844	6572	0.28	0.04849	0.00181	0.01212	0.00044	0.00181	0.00002	123	59	12.2	0.4	11.7	0.2			4%
13SW20-1 16	589	1689	0.35	0.05097	0.00462	0.01184	0.00107	0.00170	0.00004	240	162	12	1	11	0.3			9%
13SW20-1 17	463	918	0.50	0.05890	0.00777	0.01651	0.00213	0.00203	0.00006	564	299	17	2	13.1	0.4			30%
13SW20-1 18	238	3078	0.08	0.05073	0.00358	0.01624	0.00103	0.00237	0.00005	228	103	16	1	15.2	0.4			5%
13SW20-1 19	1040	1712	0.61	0.05813	0.00847	0.01090	0.00155	0.00136	0.00005	535	327	11	2	8.8	0.3			25%
13SW02-1 02	601	1101	0.55	0.05337	0.00452	0.01195	0.00093	0.00177	0.00004	345	130	12.1	0.9	11.4	0.3	9.91	0.08	6%
13SW02-1 07	431	1254	0.34	0.06226	0.00354	0.01681	0.00089	0.00206	0.00005	683	75	16.9	0.9	13.2	0.3	9.32	0.06	28%
13SW02-1 08	136	3542	0.04	0.04882	0.00230	0.01131	0.00052	0.00169	0.00003	139	72	11.4	0.5	10.9	0.2			5%
13SW02-1 11	345	2501	0.14	0.06108	0.00636	0.02098	0.00209	0.00249	0.00008	642	233	21	2	16	0.5			31%
13SW02-1 12	298	2240	0.13	0.04736	0.00313	0.01300	0.00085	0.00204	0.00004	67	107	13.1	0.9	13.2	0.3			-1%
13SW02-1 13	255	3229	0.08	0.24988	0.03570	7.89246	2.91661	0.10445	0.04514	3184	324	2219	333	640	263			247%
13SW02-1 14	1261	2077	0.61	0.06079	0.00354	0.01497	0.00080	0.00184	0.00004	632	81	15.1	0.8	11.9	0.2			27%
13SW02-1 16	791	4028	0.20	0.04415	0.00301	0.01207	0.00077	0.00201	0.00004	-63	100	12.2	0.8	12.9	0.3			-5%
13SW02-1 19	574	732	0.78	0.04605	0.00287	0.01370	0.00078	0.00216	0.00005		137	13.8	0.8	13.9	0.4			-1%
13SW02-1 20	258	3501	0.07	0.05703	0.00555	0.02020	0.00181	0.00257	0.00010	493	221	20	2	16.5	0.6			21%
13SW47-1 01	1270	3783	0.34	0.04612	0.00249	0.01066	0.00055	0.00168	0.00003	4	117	10.8	0.6	10.8	0.2			0%
13SW47-1 02	682	765	0.89	0.04606	0.00470	0.00869	0.00081	0.00137	0.00006	1	209	8.8	0.8	8.8	0.4			0%
13SW47-1 04	768	913	0.84	0.05380	0.00499	0.01289	0.00106	0.00184	0.00005	363	136	13	1	11.8	0.3			10%
13SW47-1 10	1572	5679	0.28	0.05896	0.00387	0.01880	0.00122	0.00254	0.00016	566	63	19	1	16	1			19%
13SW47-1 11	657	2809	0.23	0.04858	0.00297	0.01098	0.00067	0.00168	0.00004	128	97	11.1	0.7	10.8	0.2			3%
13SW47-1 13	449	686	0.65	0.04606	0.00591	0.01028	0.00127	0.00162	0.00005	1	241	10	1	10.4	0.3			-4%
13SW47-1 14	158	1544	0.10	0.05439	0.00373	0.42411	0.02428	0.05655	0.00214	387	159	359	17	355	13			1%
13SW47-1 17	1395	1689	0.83	0.04766	0.00306	0.00997	0.00060	0.00157	0.00005	82	82	10.1	0.6	10.1	0.3			0%
13SW49-1 04	1672	5338	0.31	0.05133	0.00258	0.01034	0.00054	0.00147	0.00003	256	77	10.4	0.5	9.5	0.2			9%

13SW49-1 06	147	1101	0.13	0.06391	0.00520	0.07453	0.00468	0.00953	0.00056	739	59	73	4	61	4			20%
13SW49-1 11	91	763	0.12	0.05093	0.00202	0.06658	0.00318	0.00953	0.00027	238	60	65	3	61	2	8.15	0.09	7%
13SW49-1 17	516	840	0.61	0.07876	0.00984	0.02231	0.00223	0.00235	0.00010	1166	134	22	2	15.1	0.6	8.93	0.08	46%
13SW49-1 19	109073	26977	4.04	0.04605	0.00332	0.00836	0.00059	0.00132	0.00002		160	8.5	0.6	8.5	0.1			0%
14QW326-2-08	277	304	0.91	0.05428	0.01154	0.01620	0.00337	0.00216	0.00009	383	414	16	3	13.9	0.6			15%
14QW326-2-10	164	356	0.46	0.05624	0.00102	0.55488	0.00973	0.07151	0.00067	462	23	448	6	445	4			1%
14QW326-2-11	1451	1260	1.15	0.05203	0.00581	0.01212	0.00133	0.00169	0.00004	287	256	12	1	10.9	0.2			10%
14QW326-2-12	264	445	0.59	0.05164	0.00549	0.30874	0.03268	0.04336	0.00046	270	244	273	25	274	3			0%
14QW326-2-14	256	355	0.72	0.04961	0.00342	0.11667	0.00785	0.01706	0.00025	177	157	112	7	109	2			3%
14QW328-3-01	122	2428	0.05	0.04379	0.00114	0.01076	0.00026	0.00179	0.00002	-81	36	10.9	0.3	11.5	0.1			-5%
14QW328-3-02	258	534	0.48	0.04919	0.00071	0.20512	0.00399	0.03016	0.00043	157	22	189	3	192	3	6.57	0.06	-2%
14QW328-3-03	350	146	2.40	0.05002	0.00605	0.04239	0.00503	0.00615	0.00014	196	266	42	5	39.5	0.9	7.38	0.09	6%
14QW328-3-04	49.5	72	0.69	0.05462	0.00147	0.42706	0.01064	0.05696	0.00063	397	36	361	8	357	4	6.06	0.1	1%
14QW328-3-05	62	119	0.52	0.06593	0.00961	0.01715	0.00241	0.00189	0.00007	804	324	17	2	12.2	0.5	9.13	0.05	39%
14QW328-3-06	189	145	1.30	0.05159	0.00818	0.01416	0.00220	0.00199	0.00006	267	324	14	2	12.8	0.4	9.83	0.09	9%
14QW328-3-07	135	142	0.95	0.04743	0.00180	0.11334	0.00402	0.01751	0.00021	71	58	109	4	112	1			-3%
14QW328-3-08	30.9	55.7	0.55	0.04847	0.00189	0.27272	0.01096	0.04082	0.00056	122	68	245	9	258	3			-5%
14QW328-3-09	99	86	1.16	0.04605	0.00662	0.15197	0.02175	0.02394	0.00032		262	144	19	152	2			-5%
14QW328-3-11	27.9	14.7	1.90	0.15203	0.02154	0.12538	0.01357	0.00763	0.00047	2369	104	120	12	49	3	6.72	0.07	145%
14QW328-3-13	173	212	0.82	0.05294	0.00129	0.25912	0.00689	0.03545	0.00045	326	37	234	6	225	3			4%
14QW328-3-14	35.3	94	0.37	0.06962	0.00307	0.73244	0.02989	0.07630	0.00127	917	93	558	18	474	8			18%
14QW328-3-18	497	2255	0.22	0.04822	0.00138	0.01900	0.00052	0.00286	0.00002	110	67	19.1	0.5	18.4	0.2			4%
14QW328-3-19	2079	43654	0.05	0.04682	0.00140	0.01082	0.00030	0.00167	0.00002	40	43	10.9	0.3	10.8	0.1			1%
14QW328-3-21	1827	2994	0.61	0.05023	0.00125	0.21256	0.00534	0.03060	0.00041	206	34	196	4	194	3			1%
14QW328-3-22	5870	6001	0.98	0.04638	0.00449	0.01347	0.00128	0.00211	0.00004	17	207	14	1	13.6	0.2			3%
14QW328-3-23	7569	5165	1.47	0.04897	0.00206	0.03853	0.00155	0.00572	0.00007	146	70	38	2	36.8	0.5			3%
14QW328-3-24	6659	5051	1.32	0.06260	0.00350	0.02419	0.00130	0.00288	0.00006	695	80	24	1	18.5	0.4			30%
14QW328-3-25	2893	3100	0.93	0.04606	0.00966	0.00986	0.00205	0.00155	0.00004	1	350	10	2	10	0.3			0%
14QW328-3-26	3265	4843	0.67	0.05571	0.00470	0.01216	0.00089	0.00169	0.00004	441	124	12.3	0.9	10.9	0.2	8.18	0.09	13%

Qinghu zircon standard for SIMS, Concordia age = 158.6 ± 2.1 Ma																	
Spot	Th ppm	U ppm	Th/U	$^{207}Pb/^{206}Pb$		$^{207}Pb/^{235}U$		$^{206}Pb/^{238}U$		$^{207}Pb/^{206}Pb$ (Ma)		$^{207}Pb/^{235}U$ (Ma)		$^{206}Pb/^{238}U$ (Ma)		Disc
				Ratio	1σ %	Ratio	1σ %	Ratio	1σ %	Age	1σ	Age	1σ	Age	1σ	
Qinghu@1	397	979	0.41	0.04917	1.36	0.16803	2.04	0.0248	1.52	155.8	31.5	157.7	3.0	157.8	2.4	-0.08%
Qinghu@2	700	1986	0.35	0.04921	0.94	0.17212	1.77	0.0254	1.50	158.0	21.8	161.3	2.6	161.5	2.4	-0.14%
Qinghu@3	309	666	0.46	0.04969	1.63	0.17218	2.22	0.0251	1.51	180.4	37.5	161.3	3.3	160.0	2.4	0.81%
Qinghu@4	813	1354	0.60	0.05050	1.69	0.16908	2.32	0.0245	1.51	198.3	40.4	158.6	3.4	156.0	2.3	1.70%
Qinghu@5	618	1112	0.56	0.04956	1.70	0.17020	2.35	0.0249	1.63	174.2	39.1	159.6	3.5	158.6	2.6	0.62%

91500 zircon standard for LA-ICP-MS, Concordia age = 1062.4 ± 5.8 Ma																
Spot	Th ppm	U ppm	Th/U	$^{207}Pb/^{206}Pb$		$^{207}Pb/^{235}U$		$^{206}Pb/^{238}U$		$^{207}Pb/^{206}Pb$ (Ma)		$^{207}Pb/^{235}U$ (Ma)		$^{206}Pb/^{238}U$ (Ma)		Disc
				Ratio	1σ	Ratio	1σ	Ratio	1σ	Age	1σ	Age	1σ	Age	1σ	
91500std	24.6	95.1	0.26	0.07561	0.00242	1.86493	0.05848	0.17876	0.00275	1085	63.7	1069	20.7	1060	15.0	2.33%
91500std	19.8	81.2	0.24	0.07415	0.00244	1.83547	0.05873	0.17958	0.00276	1056	66.7	1058	21.0	1065	15.1	-0.85%
91500std	33.1	118	0.28	0.07538	0.00213	1.86087	0.05383	0.17875	0.00248	1080	62.0	1067	19.1	1060	13.5	1.84%
91500std	26.7	103	0.26	0.07438	0.00220	1.83953	0.05382	0.17959	0.00258	1054	59.7	1060	19.2	1065	14.1	-1.03%
91500std	33.2	115	0.29	0.07527	0.00215	1.86056	0.05230	0.17876	0.00254	1076	57.4	1067	18.6	1060	13.9	1.48%
91500std	35.0	128	0.27	0.07449	0.00220	1.83984	0.04947	0.17958	0.00254	1055	63.9	1060	17.7	1065	13.9	-0.94%
91500std	17.3	75.5	0.23	0.07441	0.00281	1.84695	0.06847	0.17915	0.00289	1054	75.9	1062	24.4	1062	15.8	-0.81%
91500std	23.7	87.2	0.27	0.07535	0.00290	1.85345	0.06613	0.17919	0.00289	1080	77.8	1065	23.5	1063	15.8	1.61%
91500std	33.6	121	0.28	0.07571	0.00227	1.87396	0.05264	0.17925	0.00255	1087	59.3	1072	18.6	1063	13.9	2.28%
91500std	28.8	105	0.27	0.07405	0.00250	1.82644	0.05793	0.17909	0.00268	1043	68.5	1055	20.8	1062	14.7	-1.83%
91500std	34.2	121	0.28	0.07429	0.00212	1.82953	0.05164	0.17924	0.00223	1050	57.4	1056	18.5	1063	12.2	-1.21%
91500std	34.7	120	0.29	0.07547	0.00192	1.87087	0.05007	0.17910	0.00214	1081	51.1	1071	17.7	1062	11.7	1.80%
91500std	27.1	99	0.27	0.07319	0.00207	1.80752	0.05034	0.17921	0.00261	1020	57.4	1048	18.2	1063	14.3	-3.98%
91500std	34.2	120	0.28	0.07474	0.00196	1.84973	0.05231	0.17904	0.00248	1061	56.5	1063	18.6	1062	13.5	-0.06%
91500std	33.4	121	0.28	0.07353	0.00211	1.81240	0.05170	0.17907	0.00273	1028	59.3	1050	18.7	1062	14.9	-3.21%
91500std	19.5	76.9	0.25	0.07537	0.00238	1.85986	0.05873	0.17922	0.00291	1080	63.7	1067	20.9	1063	15.9	1.59%
91500std	22.1	84.3	0.26	0.07439	0.00222	1.84054	0.05691	0.17912	0.00283	1054	65.7	1060	20.3	1062	15.5	-0.80%
91500std	32.3	114	0.28	0.07499	0.00207	1.84996	0.05018	0.17916	0.00248	1133	55.6	1063	17.9	1062	13.5	6.68%

91500std	21.4	83.9	0.25	0.07477	0.00229	1.85044	0.05771	0.17918	0.00269	1062	62.2	1064	20.6	1062	14.7	-0.04%
91500std	27.9	102	0.27	0.07686	0.00233	1.89516	0.05712	0.17902	0.00292	1118	59.7	1079	20.0	1062	16.0	5.27%
91500std	27.2	99	0.28	0.07290	0.00215	1.80524	0.05145	0.17932	0.00241	1013	60.0	1047	18.6	1063	13.2	-4.73%
91500std	29.2	105	0.28	0.07379	0.00219	1.82374	0.05412	0.17918	0.00258	1035	59.3	1054	19.5	1063	14.1	-2.57%
91500std	31.0	113	0.27	0.07597	0.00202	1.87666	0.04990	0.17916	0.00266	1094	53.2	1073	17.6	1062	14.6	3.02%
91500std	29.4	104	0.28	0.07471	0.00222	1.84071	0.05239	0.17924	0.00282	1061	60.3	1060	18.7	1063	15.4	-0.16%
91500std	28.1	97	0.29	0.07505	0.00223	1.85969	0.05580	0.17910	0.00267	1069	59.3	1067	19.8	1062	14.6	0.69%

Note:

1. If $^{206}Pb/^{238}U$ age <1000, Disc (Discordance) = ($^{207}Pb/^{235}U$ age)/ ($^{206}Pb/^{238}U$ age)-1; If $^{206}Pb/^{238}U$ age >1000, Disc = ($^{207}Pb/^{206}Pb$ age)/ ($^{206}Pb/^{238}U$ age)-1.

2. Results described in this study exclude analyses with >10% discordance.

Table S3 In-situ LA-ICP-MS trace element (ppm) results for the zircon of granulite xenoliths entrained in 3.8 Ma trachytes.

Spot#	Introductions	La	Ce	Pr	Nd	Sm	Eu	Gd	Tb	Dy	Ho	Er	Tm	Yb	Lu	Ti	T/℃
11WL61-7: granulite xenolith																	
1	metamorphic	0.04	5.36	0.03	0.62	2.59	0.40	21.57	7.24	74.02	21.75	88.46	17.91	157.22	26.64	9.52	791.18
3	metamorphic	0.32	6.75	0.11	1.24	4.15	0.43	29.06	9.88	102.16	31.14	130.66	26.41	230.01	41.48	8.81	783.30
4	metamorphic	0.02	15.87	0.05	1.16	2.14	0.14	12.78	4.29	53.43	19.04	87.21	17.50	157.04	26.41	14.88	839.00
5	metamorphic	0.02	6.70	0.03	0.66	3.77	0.45	28.68	9.46	96.94	29.25	119.77	24.61	216.37	37.57	6.14	748.06
6	metamorphic	0.10	6.84	0.05	1.13	3.71	0.47	29.16	9.48	99.07	28.95	122.20	24.78	215.78	38.48	6.13	747.91
7	core	0.38	29.89	0.21	2.80	5.40	2.25	30.41	9.57	117.47	43.62	205.69	46.05	435.99	80.58	7.71	770.00
8	rim	0.10	6.84	0.05	1.13	3.71	0.47	29.16	9.48	99.07	28.95	122.20	24.78	215.78	38.48	6.13	747.91
11WL61-2: granulite xenolith																	
1	rim	3.48	8.49	0.80	3.86	1.98	0.16	12.58	4.64	48.25	13.93	48.63	6.90	44.13	7.41	7.10	761.95
2	rim	0.10	1.51	0.07	0.58	1.56	0.17	13.00	4.65	44.44	11.28	33.98	5.26	36.03	5.20	5.92	744.63
3	rim	5.44	9.16	0.98	4.89	4.95	0.32	27.46	7.41	56.19	10.33	24.96	3.06	18.88	2.89	6.68	756.08
5	core	0.33	9.97	0.16	1.08	2.06	0.30	12.59	5.01	69.50	28.94	161.20	40.03	427.90	77.83	302.70	1322.67
6	core	0.19	3.06	0.16	2.19	4.30	0.13	23.07	7.59	84.21	30.69	147.34	31.87	302.22	58.10	36.59	949.68
7	rim	0.09	3.27	0.09	0.56	1.27	0.28	7.92	3.20	45.26	19.78	113.27	29.91	324.36	66.29	13.69	829.75
8	metamorphic	0.62	2.08	0.21	1.09	2.37	0.25	17.89	4.97	36.31	6.90	18.40	2.60	17.78	3.11	20.66	876.97
9	metamorphic	0.14	1.98	0.08	0.76	1.76	0.19	11.10	3.22	25.15	7.74	43.49	11.44	138.60	30.52	12.09	816.24
Standard: NIST610 and NIST612																	
NIST610		435.83	449.73	446.37	431.02	455.51	454.35	478.35	441.29	446.15	456.99	461.33	443.48	461.09	443.70	453.92	
NIST610		441.96	459.26	456.50	450.14	467.80	462.75	487.97	456.35	455.00	461.96	469.58	450.35	466.48	453.19	470.28	
NIST610		443.70	452.99	447.72	433.03	456.55	447.60	453.50	438.83	441.65	453.35	458.24	436.29	451.14	444.92	452.30	
NIST610		443.65	454.10	449.50	426.63	454.65	448.66	447.88	436.55	435.27	449.07	451.64	435.59	450.56	436.17	451.02	
NIST610		437.83	453.23	447.58	425.80	448.24	444.04	433.81	430.82	430.19	449.54	457.34	432.73	448.36	437.95	447.63	
NIST610		433.55	446.18	441.27	420.14	441.50	436.26	425.81	428.25	425.12	436.37	443.54	424.14	436.29	426.67	441.65	
NIST610		436.16	448.76	443.11	420.85	442.61	435.85	433.80	428.34	424.56	435.18	445.46	423.20	437.12	432.29	440.64	
NIST610		442.43	456.59	448.40	427.97	445.54	437.51	430.55	431.34	430.27	441.82	447.18	427.07	443.90	434.19	452.70	
NIST612		34.43	36.60	36.46	33.15	36.57	34.23	37.05	36.25	34.61	36.30	36.71	35.70	37.21	35.66	45.71	

NIST612	35.00	37.18	36.99	34.71	35.78	34.12	37.42	35.11	34.72	36.38	36.46	35.33	38.13	35.28	46.41
NIST612	34.58	36.75	35.99	33.22	35.59	33.65	34.41	34.45	34.01	35.21	36.20	34.31	35.59	35.00	41.78
NIST612	35.69	37.63	36.89	33.81	36.07	34.04	34.25	34.68	33.64	35.84	36.03	34.36	36.60	35.14	37.10
NIST612	35.11	37.66	36.75	34.51	35.10	33.68	34.35	34.97	32.72	35.84	36.34	34.23	35.46	34.32	39.53
NIST612	35.24	36.94	36.79	33.55	36.33	34.06	36.44	34.88	33.80	36.16	36.46	34.58	36.93	34.54	36.87
NIST612	35.72	37.24	37.03	34.86	37.01	34.30	34.79	35.84	34.37	36.23	36.95	34.95	35.51	34.97	38.44
NIST612	35.30	37.15	36.24	34.21	36.04	34.67	35.93	35.42	33.96	35.95	36.36	35.15	36.38	34.81	35.29

Note:

1. The in-situ trace element analysis spot correspond to those of SIMS zircon U-Pb dating (Table S1).

2. In order to obtain high quality data, the zircon grains were polished slightly prior to the test, and some smaller grains (e.g., 11WL61-7@2, 11WL61-2@4) were accidentally polished out without obtaining trace data.

3. Temperatures calculated by Ti-in-zircon geothermometer assuming α_{SiO2} = 1, α_{TiO2} = 0.6 (Ferry and Watson, 2007; Watson et al., 2006)

4. Ti content of 11WL61-2@5 is very high, up to 302.70 ppm, and most probably as a result of inclusions in the zircons.

Table S4 Representative analyses of minerals of granulite xenoliths entrained in 3.8 Ma trachytes.

	11WL61-7 (mafic granulite)												11WL61-2 (mafic granulite)						
Mineral	Pl	Pl	Opx	Opx	Cpx	Cpx	Bt	Amp	Ilm	Tmt	Ilm	Tmt	Pl	Pl	Opx	Opx	Cpx	Bt	Ilm
SiO_2	54.35	53.67	51.76	51.95	52.36	51.95	36.71	42.07	0.1	0.44	0.02	0.55	56.34	54.04	51.45	52.08	50.41	36.72	0.04
TiO_2	\	\	0.05	0.12	0.25	0.19	4.77	2.36	46.82	12.65	46.8	12.68	0.01	\	0.23	0.14	0.3	6.87	49.32
Al_2O_3	27.97	28.54	3.32	3.23	2.53	2.76	14.8	12.07	0.6	9.1	0.24	5.76	26.81	28.98	5	3.51	2.82	13.93	0.18
FeO	0.37	0.53	22.29	22.84	10.93	10.77	13.01	14.84	46.65	70.45	49.1	71.98	0.08	0.44	19.95	20.81	10.76	13.14	47.25
MnO	0.04	0.02	0.09	0.09	0.04	0.03	0.05	0.10	0.34	0.42	0.53	0.33	0.01	0.01	0.91	1.01	0.31	\	1.12
MgO	0.04	0.03	21.45	21.97	13.42	13.20	15.33	10.61	3.99	4.65	1.35	4.42	0.01	0.06	22.29	22.09	13.28	14.69	1.19
CaO	11.56	12.75	0.39	0.38	20.60	20.32	0.08	11.82	0.07	0.02	\	0.09	9.37	12.08	0.81	0.74	21.02	0.16	\
Na_2O	4.38	4.26	0.13	0.02	0.48	0.55	0.63	1.72	0.07	0.04	0.28	0.08	6.28	4.3	0.07	0.12	0.73	1.22	0.1
K_2O	0.67	0.49	\	\	0.01	0.01	9.96	1.67	\	0.07	0.01	0.16	0.95	0.77	\	0.01	\	8.35	0.02
F	\	\	\	\	\	\	\	\	\	\	\	\	0.01	\	\	\	\	2.56	\
Cl	0.01	\	0.01	\	0.00	0.01	0.01	0.03	\	\	0.03	\	0.03	0.01	\	0.01	\	0.20	0.02
Total	99.39	100.28	99.48	100.59	100.61	99.78	95.34	97.27	98.64	97.84	98.35	96.04	99.9	100.68	100.71	100.51	99.63	97.83	99.23
Oxygens	8	8	6	6	6	6	11	23	3	4	3	4	8	8	6	6	6	11	3
Si	2.482	2.441	1.932	1.922	1.948	1.947	2.736	6.335	0.003	0.017	0.001	0.023	2.547	2.437	1.886	1.921	1.908	2.654	0.001
Ti	\	\	0.001	0.003	0.007	0.005	0.268	0.267	0.902	0.372	0.921	0.391	\	\	0.006	0.004	0.009	0.373	0.952
Al	1.505	1.530	0.146	0.141	0.111	0.122	1.3	2.142	0.018	0.42	0.007	0.278	1.429	1.541	0.216	0.153	0.126	1.187	0.005
Fe^{3+}	\	\	0.000	0.000	0.021	0.020	0.135	0.265	0.257	1.085	0.242	1.208	\	\	0.008	0.01	0.14	0.455	0.132
Fe^{2+}	\	\	0.698	0.706	0.318	0.317	0.675	1.603	0.743	1.219	0.833	1.256	\	\	0.603	0.631	0.196	0.339	0.882
Mn	\	\	0.003	0.003	0.001	0.001	0.003	0.012	0.007	0.014	0.012	0.012	\	\	0.028	0.031	0.01	0.000	0.024
Mg	\	\	1.181	1.212	0.744	0.737	1.703	2.381	0.152	0.271	0.053	0.27	\	\	1.218	1.214	0.749	1.583	0.046
Ca	0.566	0.602	0.016	0.015	0.821	0.816	0.006	1.906	0.002	0.001	\	0.004	0.454	0.584	0.032	0.029	0.852	0.012	
Na	0.388	0.386	0.010	0.001	0.034	0.040	0.091	0.503	0.003	0.003	0.014	0.006	0.551	0.376	0.005	0.009	0.053	0.171	0.005
K	0.039	0.028	0.000	0.000	0.000	0.001	0.947	0.32	\	0.004	\	0.008	0.055	0.044	\	\	\	0.770	0.001
An (Pl)	57.0	59.2	\	\	\	\	\	\	\	\	\	\	42.8	58.2	\	\	\	\	\
Mg#(Opx)	\	\	62.8	63.2	\	\	\	\	\	\	\	\	\	\	66.6	65.4	69.0	66.6	\
	Titanomagnetite-Ilmenite thermometer (Sauerzapf et al., 2008): **829–884 ℃**																		

Note: An = Ca/ (Ca + Na +K) ×100%; Mg# (Opx) = Mg/ (Mg + Fe^{2+}) ×100%

Table S5 Representative analyses of minerals of amphibolite facies xenoliths contained in 28 Myr syenites porphyries.

	11GM01-20 (garnet amphibolite)					11GM01-10 (garnet amphibolite)						11GM01-21 (amphibolite)		
mineral	grt	cpx	amp	pl	pl	cpx	pl	amp	grt	cpx	bt	amp	pl	bt
SiO_2	38.23	51.45	42.33	53.02	51.59	51.32	52.94	42.98	38.32	51.37	36.04	43.13	59.32	36.36
TiO_2	0.1	0.19	2.01	\	\	0.16	\	2.19	0.02	0.12	3.74	2.27	0.03	5.12
Al_2O_3	21.52	1.98	12.14	29.17	29.76	1.66	28.5	12.57	21.71	1.76	16.81	12.24	25.37	14.6
FeO	25.68	10.18	14.88	0.11	0.03	9.58	0.13	13.16	26.74	9.43	16.68	14.46	\	18.01
MnO	0.86	0.22	0.09	0.04	\	0.16	0.03	0.1	1.4	0.12	0.14	0.07	\	0.12
MgO	6.33	12.34	10.67	0.01	0.01	12.6	\	10.97	6.32	12.43	12.61	10.17	0.01	12.14
CaO	6.85	23.17	12.08	12.31	13.48	24	11.89	12.33	6.3	23.89	\	12.29	7.13	\
Na_2O	0.03	0.73	1.68	5.13	4.43	0.73	5.23	1.62	\	0.7	0.61	1.89	7.98	0.65
K_2O	0.01	0.09	1.6	0.29	0.24	\	0.32	1.61	\	0.03	9.3	1.57	0.28	8.99
F	\	\	\	0.01	\	\	\	\	\	\	\	\	b.d.	\
Cl	\	0.01	0.02	\	0.01	0.01	\	0.07	0.01	0.01	0.12	0.08	0.01	0.02
Total	99.61	100.36	97.51	100.08	99.56	100.22	99.04	97.61	100.82	99.86	96.05	98.17	100.11	96
Oxygens	12	6	23	8	8	6	8	23	12	6	11	23	8	11
Si	2.982	1.937	6.356	2.409	2.362	1.935	2.428	6.386	2.966	1.941	2.698	6.413	2.65	2.742
Ti	0.006	0.005	0.227	\	\	0.004	\	0.245	0.001	0.003	0.211	0.254	0.001	0.291
Al	1.978	0.088	2.147	1.562	1.606	0.074	1.541	2.202	1.981	0.078	1.483	2.144	1.335	1.298
Fe^{3+}	0.029	0.126	0.261	\	\	0.151		0.354	0.041	0.128	0.17	0.327	\	0.203
Fe^{2+}	1.646	0.191	1.608	0.004	0.001	0.148	0.005	1.281	1.689	0.167	0.875	1.471	\	0.933
Mn	0.057	0.007	0.012	0.002	\	0.005	0.001	0.013	0.092	0.004	0.009	0.008	\	0.008
Mg	0.736	0.693	2.389	\	\	0.708	\	2.43	0.73	0.7	1.408	2.255	\	1.365
Ca	0.573	0.935	1.943	0.599	0.661	0.969	0.584	1.963	0.523	0.967	\	1.957	0.341	\
Na	0.005	0.053	0.489	0.452	0.393	0.054	0.465	0.468	\	0.051	0.089	0.545	0.691	0.094
K	\	0.004	0.307	0.017	0.014	\	0.019	0.305	\	0.001	0.889	0.299	0.016	0.865
Grt-Cpx Thermometer (Ravna, 2000)	**664 ℃**					**620 ℃**						\		
Amp-Pl Thermometer (Holland and Blundy, 1994)	**730 ℃**					**640 ℃**						**627 ℃**		

Grt-Cpx-Pl-Qtz Barometer (Eckert et al., 1991)	**10 kbar**	**9 kbar**	\
Grt-Cpx-Pl-Qtz Barometer (Newton and Perkins, 1982)	**8 kbar**	**7 kbar**	\

References

Andersen, T., 2002, Correction of common lead in U–Pb analyses that do not report 204Pb: Chemical Geology, v. 192, p. 59–79.

Eckert, J.O., Newton, R.C., Kleppa, O.J., 1991, The H of reaction and recalibration of garnet–pyroxene–plagioclase–quartz geobarometers in the CMAS system by solution calorimetry: American Mineralogist, v. 76, n. 1–2, p. 148–160.

Ferry J.M., Watson E.B., 2007, New thermodynamic models and revised calibrations for the Ti-in-zircon and Zr-inrutile thermometers: Contrib Mineral Petrol, v. 154, p. 429–437.

Green, E. C. R., White, R. W., Diener, J. F. A., Powell, R., Holland, T. J. B., & Palin, R. M., 2016, Activity–composition relations for the calculation of partial melting equilibria for metabasic rocks: Journal of Metamorphic Geology, v. 34, p. 845–869.

Hacker, B. R., and Abers G. A., Subduction Factory 3, 2004, An Excel worksheet and macro for calculating the densities, seismic wave speeds, and H_2O contents of minerals and rocks at pressure and temperature: Geochemistry Geophysics Geosystems, v. 5, Q01005.

Holland, T., & Blundy, J., 1994, Non-ideal interactions in calcic amphiboles and their bearing on amphibole-plagioclase thermometry: Contributions to mineralogy and petrology, v. 116, n. 4, p. 433-447.

Holland, T.J.B. & Powell, R., 2003, Activity–composition relations for phases in petrological calculations: an asymmetric multicomponent formulation: Contributions to Mineralogy and Petrology, v. 145, p. 492–501.

Holland, T.J.B. & Powell, R., 2011, An improved and extended internally consistent thermodynamic dataset for phases of petrological interest, involving a new equation of state for solids: Journal of Metamorphic Geology, v. 29, p. 333–383.

Jackson, S.E., Pearson, N.J., Belousova, E., Griffin, W.L., 2004, The application of laser ablation-inductively coupled plasma-mass spectrometry (LA-ICP-MS) to in situ U– Pb geochronology: Chemical Geology, v. 211, p. 47–69.

Li, X. H., Long, W. G., Li, Q. L., Liu, Y., Zheng, Y. F., Yang, Y. H., Chamberlain, K. R., Wan, D. F., Guo, C. H., Wang, X. C., and Tao, H., 2010, Penglai Zircon Megacrysts: A Potential New Working Reference Material for Microbeam Determination of Hf-O Isotopes and U-Pb Age: Geostandards and Geoanalytical Research, v. 34, no. 2, p. 117–134.

Li, X., Tang, G., Gong, B., Yang, Y., Hou, K., Hu, Z., Li, Q., Liu, Y., and Li, W., 2013, Qinghu zircon: A working reference for microbeam analysis of U-Pb age and Hf and O isotopes: Chinese Science Bulletin, v. 58, p. 4647–4654.

Li, X.H., Liu, Y., Li, Q.L., Guo, C.H., and Chamberlain, K.R., 2009, Precise determination of Phanerozoic zircon Pb/Pb age by multicollector SIMS without external standardization: Geochemistry, Geophysics, Geosystems, v. 10, Q04010.

Ludwig, K. R., 2003, User's Manual for Isoplot/Ex Version 3.00. In: Ludwig, K. R., ed., A Geochronological Toolkit for Microsoft Excel. Berkeley Geochronology Center Special

Publication: Berkeley, p. 41–70.

Newton, R.C., Perkins, D., 1982, Thermodynamic calibration of geobarometers based on the assemblages garnet–plagioclase–orthopyroxene (clinopyroxene) –quartz. American Mineralogist: v. 67, no. 2, p. 203–222.

Ou, Q., 2017, Middle Eocene-Late Miocene (42-6 Ma) igneous rocks in Gemuchaka-Chibuzhangcuo area, Qiangtang Block (central Tibet Plateau): Petrogenesis and insights for deep geodynamics, [Ph.D. thesis]: University of Chinese Academy of Sciences, 380 p (in Chinese with English abstract).

Palin, R.M., White, R.W., Green, E.C.R., Diener, J.F.A., Powell, R., Holland, T.J.B., 2016, Highgrade metamorphism and partial melting of basic and intermediate rocks: J. Metamorph. Geol., v. 34, p. 871–892.

Powell, R. & Holland, T.J.B., 1988, An internally consistent dataset with uncertainties and correlations: 3. Applications to geobarometry, worked examples and a computer program: Journal of Metamorphic Geology, v. 6, p. 173–204.

Ravna, E.K., 2000, Distribution of Fe^{2+} and Mg between coexisting garnet and hornblende in synthetic and natural systems: an empirical calibration of the garnet–hornblende Fe–Mg geothermometer: Lithos, v. 53, no. 3–4, p. 265–277.

Sauerzapf, U., Lattard, D., Burchard, M., Engelmann, R., 2008, The titanomagnetite-ilmenite equilibrium: new experimental data and thermo-oxybarometric application to the crystallization of basic to intermediate rocks: J. Petrol., v. 49, 1161e1185

Sláma, J., Košler, J., Condon, D. J., Crowley, J. L., Gerdes, A., Hanchar, J. M., Horstwood, M. S. A., Morris, G. A., Nasdala, L., Norberg, N., Schaltegger, U., Schoene, B., Tubrett, M. N., Whitehouse, M. J., 2008, Plešovice zircon – a new natural reference material for U-Pb and Hf isotopic microanalysis: Chemical Geology, v. 249, p. 1–35.

Sun, S.S., McDonough, W.F., 1989, Chemical and isotopic systematics of oceanic basalts: implications for mantle composition and processes: Geological Society, London, Special Publications, p. 313–345.

Watson, E.B., Wark, D.A., Thomas, J., 2006, Crystallization thermometers for zircon and rutile: Contrib. Mineral. Petrol., v. 151, n. 4, p. 413–433.

White, R.W., Powell, R. & Clarke, G.L., 2002, The interpretation of reaction textures in Fe-rich metapelitic granulites of the Musgrave Block, central Australia: constraints from mineral equilibria calculations in the system K_2O–FeO–MgO–Al_2O_3–SiO_2–H_2O–TiO_2–Fe_2O_3: Journal of Metamorphic Geology, v. 20, p. 41–55.

White, R.W., Powell, R. & Johnson, T.E., 2014, The effect of Mn on mineral stability in metapelites revisited: new a–x relations for manganese-bearing minerals: Journal of Metamorphic Geology, v. 32, p. 809–828.

White, R.W., Powell, R., Holland, T.J.B. & Worley, B.A., 2000, The effect of TiO_2 and Fe_2O_3 on metapelitic assemblages at greenschist and amphibolite facies conditions: mineral equilibria calculations in the system K_2O–FeO–MgO–Al_2O_3–SiO_2–H_2O–TiO_2–Fe_2O_3: Journal of Metamorphic Geology, v. 18, p. 497–511.

White, R.W., Powell, R., Holland, T.J.B., Johnson, T.E. & Green, E.C.R., 2014, New mineral activity–composition relations for thermodynamic calculations in metapelitic systems: Journal of Metamorphic Geology, v. 32, p. 261–286.

Wiedenbeck, M., Allé, P., Corfu, F., Griffin, W.L., Meier, M., Oberli, F., von Quadt, A., Roddick, J.C., Spiegel, W., 1995, Three natural zircon standards for U–Th–Pb, Lu–Hf, trace element and REE analyses: Geostandards and Geoanalytical Research, v. 19, p. 1–23.

Zhang, L., Ren, Z.-Y., Xia, X.-P., Yang, Q., Hong, L.-B., & Wu, D., 2019, In situ determination of trace elements in melt inclusions using laser ablation-inductively coupled plasma-sector field-mass spectrometry: Rapid Communications in Mass Spectrometry, v. 33, p. 361– 370.